Vol 17 No 5, May 2008
1674-1056/2008/17(05)/1691-07

Chinese Physics B

© 2008 Chin. Phys. Soc.
and IOP Publishing Ltd

Bifurcation analysis and control of periodic solutions changing into invariant tori in Langford system*

Liu Su-Hua(刘素华)[a)b)†], Tang Jia-Shi(唐驾时)[a)], Qin Jin-Qi(秦金旗)[a)], and Yin Xiao-Bo(尹小波)[c)]

[a)] *College of Mechanics and Aerospace, Hunan University, Changsha* 410082, *China*
[b)] *Anyang Institute of Technology, Anyang* 455000, *China*
[c)] *School of Geoscience and Environmental Engineering, Central South University, Changsha* 410083, *China*

(Received 26 July 2007; revised manuscript received 29 November 2007)

Bifurcation characteristics of the Langford system in a general form are systematically analysed, and nonlinear controls of periodic solutions changing into invariant tori in this system are achieved. Analytical relationship between control gain and bifurcation parameter is obtained. Bifurcation diagrams are drawn, showing the results of control for secondary Hopf bifurcation and sequences of bifurcations route to chaos. Numerical simulations of quasi-periodic tori validate analytic predictions.

Keywords: Langford system, nonlinear control, secondary Hopf bifurcation, torus
PACC: 0547

1. Introduction

The dynamics and bifurcation control in problems governed by three-dimensional autonomous differential systems have been greatly interested in the past two decades. Dynamics of three-dimensional systems near one of their periodic orbits is very rich in terms of bifurcation and its stability. When a periodic solution becomes unstable, stability may be transferred to a stable period-doubling motion with exactly twice or more the period of the given orbit, or to a stable quasi-periodic motion with two fundamental periods, which can be represented on a two-dimensional torus.[1] Systems undergoing a sequence of period-doubling or quasi-periodic bifurcations will result in chaotic motion. Investigations have been made about period-doubling bifurcation,[2] quasi-period tori[3−5] and route to chaos.[6] In modern nonlinear dynamics bifurcation control plays an important role.[7] Controllers can be designed to shift the location of bifurcation point, to change the stability of bifurcation and to modify the amplitude of limit cycle, etc.[8] Several methods for bifurcation control have recently been presented.[9−11] Either letting a periodic orbit transform to a torus or a torus be delayed for certain bifurcation parameters can be achieved by control with a proper choice of control gains.

The Langford system was originally proposed by Hopf[12] as a possible model for describing fluid dynamic turbulence and is a three-dimensional system with high degree of symmetry. Studies indicate that the Langford system has very rich bifurcation behaviours. A good qualitative analysis of the regular motion in the Langford system is given in Ref.[13] and its chaotic behaviour is studied in Ref.[14]. First Hopf bifurcation analysis and control via linear state feedback have been investigated in our previous work.[15] All these researches include only one set of parameters. In the present work, however, we will analyse the secondary Hopf bifurcation, i.e. the bifurcation solutions of the periodic solution, and manage to control it by a nonlinear controller without changing the location of the first Hopf bifurcation. And then, we study a general form of the Langford system and discuss in detail with another set of system parameters.

Static and dynamic bifurcations in the Langford system will be analysed in the next section. A nonlinear control of periodic solutions into invariant tori is designed and parameter–gain curves predicting sec-

*Project supported by the National Natural Science Foundation of China (Grant No 10672053).
†Corresponding author. E-mail: liusuhua968@yahoo.com.cn

ondary Hopf bifurcation are drawn in Section 3. Section 4 presents bifurcation diagrams and simulations of quasi-periodic bifurcations for the controlled system. Finally, conclusion is given in Section 5.

2. Bifurcation analysis

The Langford system in a general form is described as

$$\begin{aligned}\dot{x}_1 &= (\mu - a)x_1 - bx_2 + x_1x_3 + cx_1(1 - x_3^2),\\ \dot{x}_2 &= bx_1 + (\mu - a)x_2 + x_2x_3 + cx_2(1 - x_3^2),\\ \dot{x}_3 &= \mu x_3 - (x_1^2 + x_2^2 + x_3^2).\end{aligned} \tag{1}$$

where μ is the bifurcation parameter, a, b and c are system parameters in real numbers of $a > 0$, $b > 0$, $c > 0$. Its bifurcation characteristics will be analysed in the following subsection.

2.1. Static bifurcation

It is easy to find that system (1) has two equilibrium points: $E_0 = (0, 0, 0)$ and $E_1 = (0, 0, \mu)$.

The Jacobian $L_0(\mu)$ of system (1) at the equilibrium point E_0 is

$$L_0(\mu) = \begin{pmatrix} \mu - a & -b & 0\\ b & \mu - a & 0\\ 0 & 0 & \mu \end{pmatrix}, \tag{2}$$

with the corresponding eigenvalues $\lambda_{1,2} = \mu - a + c \pm \mathrm{i}b$, $\lambda_3 = \mu$.

At the equilibrium point E_1 the Jacobian $L_1(\mu)$ of system (1) is

$$L_1(\mu) = \begin{pmatrix} 2\mu - a + c(1 - \mu^2) & -b & 0\\ b & 2\mu - a + c(1 - \mu^2) & 0\\ 0 & 0 & -\mu \end{pmatrix}, \tag{3}$$

which has a pair of complex conjugate eigenvalues $\lambda_{1,2} = \alpha(\mu) \pm \mathrm{i}\omega(\mu)$ with $\alpha(\mu) = 2\mu - a + c(1 - \mu^2)$ and $\omega(\mu) = b$ and a real eigenvalue $\lambda_3(\mu) = -\mu$.

When $a - c > 0$, for $\mu < \mu^* = 0$ the equilibrium point E_0 is stable while the equilibrium point E_1 is unstable; but for $\mu > \mu^* = 0$, E_0 becomes unstable while E_1 turns to be stable before the first Hopf bifurcation occurs. Therefore, $(0, 0, 0; 0)$ is a static bifurcation point and system (1) exhibits a transcritical bifurcation (see Fig.3 at the end of section 2).

2.2. First Hopf bifurcation

At the equilibrium point E_0, system (1) has a pair of purely imaginary eigenvalues and a real eigenvalue for $\mu = \mu_0 = a - c$, where first Hopf bifurcation takes place. While for $a - c > 0$, it exhibits an unstable Hopf bifurcation; when $a - c < 0$, it exhibits a stable Hopf bifurcation.

At the equilibrium point E_1, system (1) undergoes a first Hopf bifurcation for some value $\mu = \mu_0$ when satisfying

$$\begin{aligned}&2\mu - a + c(1 - \mu^2) = 0,\\ &-\mu < 0,\\ &1 - c\mu \neq 0.\end{aligned} \tag{4}$$

A family of limit cycles will emerge from the bifurcation point $(0, 0, \mu_0; \mu_0)$. Solving Eq.(4), we have:
(FH1) If $c = 0$, then the first Hopf bifurcation value is $\mu = \mu_0 = \dfrac{1}{2}a$.
(FH2) If $c \neq 0$ and simultaneously $c < a < \dfrac{1 + c^2}{c}$, then the first Hopf bifurcation value is

$$\mu = \mu_0 = \frac{1}{c}(1 - \sqrt{1 - ac + c^2}).$$

Note that we do not concern with another solution

$$\mu = \mu_0 = \frac{1}{c}(1 + \sqrt{1 - ac + c^2}),$$

because it corresponds to an unstable Hopf bifurcation. Setting $a = 3$, $c = 0.2$, results in $\mu_0 = 5 - \sqrt{11} \doteq 1.6834$. Figure 1 shows the numerical simulation of limit cycles in system (1) with $a = 3$, $b = 0.25$, $c = 0.2$, $\mu = 1.72$.

For μ_0 presented in FH1 and FH2, $\alpha'(0) = 2(1 - c\mu_0) > 0$ is easily deduced from $\alpha(\mu) = 2\mu - a + c(1 - \mu^2)$ and the stability index $\beta_2 = -\dfrac{2(1 - 2c\mu_0)}{\mu_0} < 0$ is obtained according to the theory of Hopf bifurcation.[1] So the first Hopf bifurcation is supercritical and the limit cycle is stable at the bifurcation point $(0, 0, \mu_0; \mu_0)$.

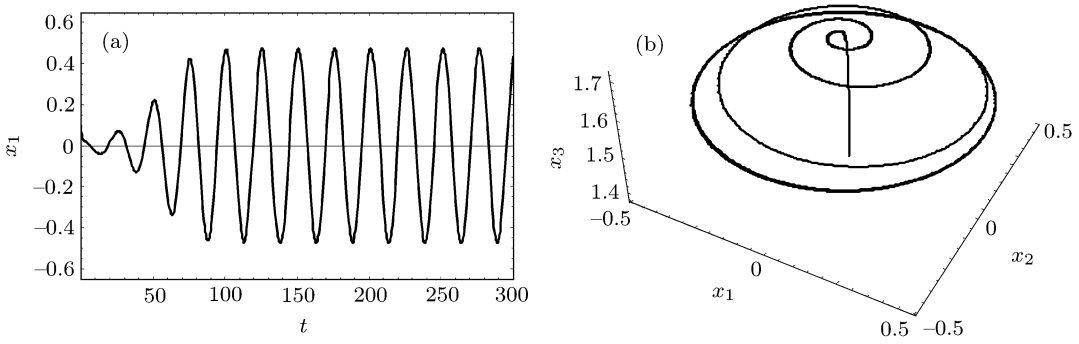


Fig.1. Numerical simulation of limit cycles in system (1) with $a = 3$, $b = 0.25$, $c = 0.2$ and $\mu = 1.72$. (a) Time–displacement curve, (b) 3D phase space trajectory.

2.3. Secondary Hopf bifurcation

When the periodic solution becomes unstable, the motion may be transferred to a quasi-periodic one, and a secondary Hopf bifurcation takes place; also a two-dimensional torus emerges from the periodic solution to substitute the limit cycle. In order to determine or modify the location of the secondary Hopf bifurcation, we manage to find the critical value of the bifurcation parameter μ at which the periodic solution gives birth to bifurcation solution, the Hopf bifurcation loses its stability and the limit cycle changes from stable to unstable. Due to the special symmetry of the Langford system, we can use a polar coordinate transformation to obtain the exact value of the secondary Hopf bifurcation.

In cylindrical coordinates $x_1 = r\cos\theta$, $x_2 = r\sin\theta$, $x_3 = x_3$, system (1) becomes

$$\begin{aligned} \dot{r} &= (\mu - a + c)r + x_3 r - c x_3^2 r, \\ \dot{\theta} &= b, \\ \dot{x}_3 &= \mu x_3 - r^2 - x_3^2. \end{aligned} \tag{5}$$

Ignoring the equation for θ and letting $\dot{r} = 0$, $\dot{x}_3 = 0$ with checking that the value of r^2 is positive, we find the equilibrium solution (r_0, x_{30}) in the plane (r, x_3), which corresponds to the limit cycle.

(i) If $c = 0$, then the equilibrium solution (r_0, x_{30}) of system (5) is

$$\begin{aligned} x_{30} &= a - \mu, \\ r_0 &= \sqrt{(a-\mu)(2\mu - a)}. \end{aligned} \tag{6}$$

(ii) If $c \neq 0$, then the equilibrium solution (r_0, x_{30}) of system (5) is

$$\begin{aligned} x_{30} &= \frac{1}{2c}(1 - \sqrt{1 + 4c(\mu - a + c)}), \\ r_0 &= \frac{1}{2c}\sqrt{4ac - 4c^2 - 2c\mu - 2 + 2(1 - c\mu)\sqrt{1 + 4c(\mu - a + c)}}. \end{aligned} \tag{7}$$

Setting $a = 3$, $c = 0.2$, the equilibrium solution is written as

$$\begin{aligned} x_{30} &= \frac{1}{2}(5 - \sqrt{20\mu - 31}), \\ r_0 &= \sqrt{\tfrac{1}{2}(3 - 5\mu + (5 - \mu)\sqrt{20\mu - 31})}. \end{aligned} \tag{8}$$

Now we consider the Jacobian of system (5) at (r_0, x_{30}) to look for the value of μ at which the stability of the equilibrium solution (r_0, x_{30}) changes. Neglecting the equation for θ, the Jacobian is written as:

$$DF(r_0, x_{30}) = \begin{pmatrix} 0 & r_0 - 2cr_0 x_{30} \\ -2r_0 & \mu - 2x_{30} \end{pmatrix}. \tag{9}$$

The corresponding characteristic equation is

$$\lambda^2 - (\mu - 2x_{30})\lambda + 2r_0^2(1 - 2cx_{30}) = 0. \tag{10}$$

According to the Routh–Hurwitz criterion the first Hopf bifurcation loses its stability and system (1)

exhibits a secondary Hopf bifurcation for some value $\mu = \mu_{00}$ when

$$\begin{aligned} &\mu - 2x_{30} = 0, \\ &1 - 2cx_{30} > 0. \end{aligned} \tag{11}$$

By consulting the first equation of Eqs.(6) and (7) it is obvious that the inequality in Eq.(11) can be satisfied for both $c = 0$ and $c \neq 0$. The solutions of the first equation in Eq.(11) are as follows:

(i) If $c = 0$, then $\mu = \mu_{00} = \frac{2}{3}a$, which is the secondary Hopf bifurcation value.

(ii) If $c \neq 0$ and simultaneously $c < a < \frac{1+c^2}{c}$, then, by inspection, the secondary Hopf bifurcation value is $\mu = \mu_{00} = \frac{1}{c}(3 - \sqrt{9 - 4ac + 4c^2})$. Setting $a = 3$, $c = 0.2$, results in $\mu_{00} = 2.0$. Figure 2 shows the numerical simulation of a torus in system (1) with $a = 3$, $b = 0.25$, $c = 0.2$ and $\mu = 2.0$.

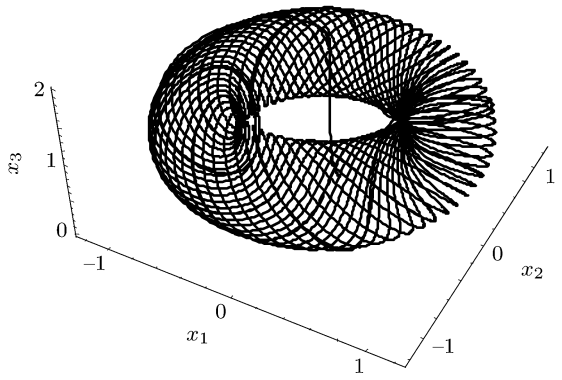


Fig.2. Tori in system (1) with $a = 3$, $b = 0.25$, $c = 0.2$, $\mu = 2.0$.

A global bifurcation diagram for system (1) with $a = 3$, $b = 0.25$, $c = 0.2$ is depicted in Fig.3 where solid lines indicate the stable static- and dynamic-state solutions, dashed lines indicate unstable static-state solutions, small dots indicate the unstable periodic solutions (limit cycles) and large dots indicate the quasi-periodic solutions (tori). At $\mu^* = 0$ a static transcritical bifurcation occurs. For $\mu_0 = 1.6834$ and $\mu_0 = 2.8$ the first Hopf bifurcation takes place corresponding to the equilibrium points $E_1 = (0, 0, \mu)$ and $E_0 = (0, 0, 0)$, respectively; the former is stable and the latter is unstable. For $\mu_{00} = 2.0$ the limit cycle from the equilibrium point $E_1 = (0, 0, \mu)$ loses its stability and the secondary Hopf bifurcation gives rise to a torus.

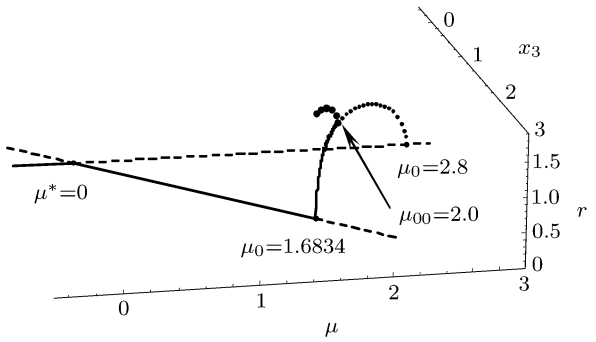


Fig.3. A global bifurcation diagram for system (1) with $a = 3$, $b = 0.25$, $c = 0.2$.

3. Nonlinear control

In order to keep the first Hopf bifurcation value unchanged, a nonlinear controller is determined as $\boldsymbol{u}(\boldsymbol{x}, \mu) = (u_1, u_2, 0)^{\mathrm{T}}$ with $u_1 = k(x_1^3 + x_1 x_2^2)$ and $u_2 = k(x_2^3 + x_1^2 x_2)$, where k is a control gain. Using this kind of controller, the control results can be exactly predicted by the approach for the uncontrolled system (1) as before.

The controlled system is written as

$$\begin{aligned} \dot{x}_1 =& (\mu - a)x_1 - bx_2 + x_1x_3 + cx_1(1 - x_3^2) \\ &+ k(x_1^3 + x_1x_2^2), \\ \dot{x}_2 =& bx_1 + (\mu - a)x_2 + x_2x_3 + cx_2(1 - x_3^2) \\ &+ k(x_2^3 + x_1^2x_2), \\ \dot{x}_3 =& \mu x_3 - (x_1^2 + x_2^2 + x_3^2). \end{aligned} \tag{12}$$

By the polar coordinate transformation $x_1 = r\cos\theta$, $x_2 = r\sin\theta$, $x_3 = x_3$, system (12) becomes

$$\begin{aligned} &\dot{r} = (\mu - a + c)r + x_3 r - cx_3^2 r + kr^3, \\ &\dot{\theta} = b, \\ &\dot{x}_3 = \mu x_3 - r^2 - x_3^2. \end{aligned} \tag{13}$$

The equilibrium solution of system (13) in the plane (r, x_3), corresponding to its periodic solution, is written as (as r^2 is positive)

$$\begin{aligned} x_{30} &= \frac{1 + \mu k - \sqrt{\Psi}}{2(c + k)}, \\ r_0^2 &= \frac{-1 + 2ac - 2c^2 - c\mu + (2a - 2c - 3\mu + c\mu^2)k + (1 - c\mu)\sqrt{\Psi}}{2(c + k)^2}, \end{aligned} \qquad (k \neq 0) \tag{14}$$

where

$$\Psi = 1 + 4c(c - a + \mu) + 2(c - 2a + 3\mu)k + \mu^2 k^2. \tag{15}$$

When $k = 0$, the equilibrium solution (14) turns to the solution (6) or (7), which is associated with the uncontrolled system (1).

Setting $a = 3$, $c = 0.2$, the equilibrium solution is given by

$$\begin{aligned} x_{30} &= \frac{5(1+\mu k) - \sqrt{-31 + 20\mu - 10(28 - 15\mu)k + 25\mu^2 k^2}}{2(1+5k)}, \\ r_0^2 &= \frac{3 - 5\mu + 5(28 - 15\mu + \mu^2)k + (5-\mu)\sqrt{-31 + 20\mu - 10(28 - 15\mu)k + 25\mu^2 k^2}}{2(1+5k)^2}. \end{aligned} \tag{16}$$

Ignoring the equation for θ, the Jacobian of the controlled system (13) at the equilibrium solution (r_0, x_{30}) is derived as:

$$DF_k(r_0, x_{30}) = \begin{pmatrix} 2r_0^2 k & r_0 - 2cx_{30}r_0 \\ -2r_0 & \mu - 2x_{30} \end{pmatrix}. \tag{17}$$

The corresponding characteristic equation is

$$\begin{aligned} &\lambda^2 + (2x_{30} - \mu - 2r_0^2 k)\lambda + 2(1 - 2cx_{30})r_0^2 \\ &+ 2r_0^2(\mu - 2x_{30})k = 0. \end{aligned} \tag{18}$$

Based on the Routh–Hurwitz criterion, the condition that the controlled system, for some value $\mu = \mu_{00}$, undergoes a secondary Hopf bifurcation is

$$\begin{aligned} &2x_{30} - \mu - 2r_0^2 k = 0, \\ &1 - 2cx_{30} + (\mu - 2x_{30})k > 0. \end{aligned} \tag{19}$$

Substituting the solution (14) into Eq.(19), yields

$$k = \frac{-4a + 4c + 6\mu + 2ac\mu - 2c^2\mu - 3c\mu^2 + 2(-2a + 2c + 3\mu - c\mu^2)\sqrt{1 - ac + c^2 + \frac{1}{2}c\mu}}{4a^2 - 8ac + 4c^2 - 12a\mu + 12c\mu + 5\mu^2 + 4ac\mu^2 - 4c^2\mu^2 - 2c\mu^3}, \tag{20}$$

which is the relationship between the parameters and the control gain when the secondary Hopf bifurcation takes place. Setting $a = 3$, $c = 0.2$, we have

$$k = \frac{280 - 178\mu + 15\mu^2 + (28 - 15\mu + \mu^2)\sqrt{44 + 10\mu}}{-784 + 840\mu - 181\mu^2 + 10\mu^3}, \tag{21}$$

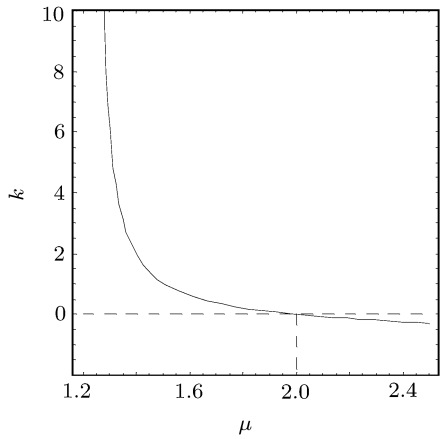


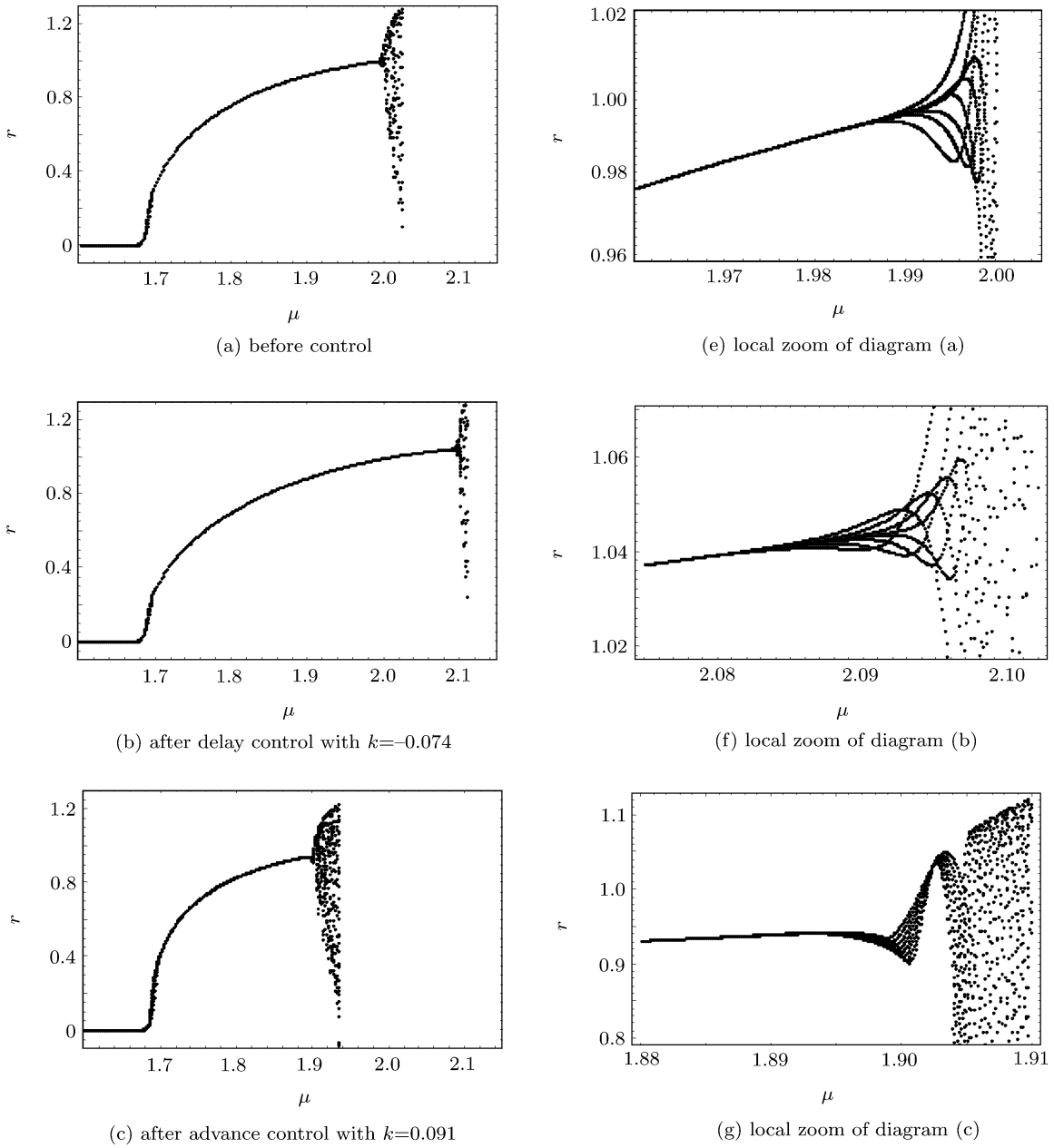
Fig.4. Parameter gain $(\mu - k)$ curves for system (12) with $a = 3$, $b = 0.25$, $c = 0.2$ undergoing a secondary Hopf bifurcation.

according to which we can determine the control gain k such that the predicted secondary Hopf bifurcation point can be delayed or advanced to a desired value, e.g. for a delayed bifurcation value $\mu = \mu_{00} = 2.1$ predicted, the control gain k should be chosen as $k = -0.074$ and for the advanced $\mu = \mu_{00} = 1.9$, we calculate $k = 0.091$. The parameter–gain $(\mu - k)$ curve of Eq.(21) is drawn in Fig.4.

4. Simulation

In this section we will give some numerical simulations for the controlled system (12). All considerations here are with respect to the set of parameters $a = 3$,

$b = 0.25$, $c = 0.2$. Figure 5 shows that the secondary Hopf bifurcation value is changed from $\mu_{00} = 2.0$ to $\mu_{00} = 2.1$ (see Fig.5(b)), delaying the chaotic motion of the uncontrolled system, or to $\mu_{00} = 1.9$ (see Fig.5(c)), advancing the original chaotic motion. The locally zooming diagrams of Figs.5(a)–5(c) are respectively drawn in Figs.5(e)–5(g) in turn so as to show the secondary Hopf bifurcation more clear. We can see that the control will keep the first Hopf bifurcation point in the uncontrolled system unchanged.



(a) before control

(e) local zoom of diagram (a)

(b) after delay control with k=–0.074

(f) local zoom of diagram (b)

(c) after advance control with k=0.091

(g) local zoom of diagram (c)

Fig.5. Secondary Hopf bifurcation delay or advance via nonlinear feedback control in system (12) with $a = 3$, $b = 0.25$, $c = 0.2$.

To validate the analytic prediction of the control, the trajectory of the controlled system (12) is numerically simulated with different choices of the control gain and the bifurcation parameter. With $k = -0.074$ and $\mu = 2.093$, the latter of which is close to the secondary Hopf bifurcation value $\mu_{00} = 2.1$, there is a torus in the phase portrait (see Fig.6) and the limit cycle remains in the controlled system (12) with $k = -0.074$ and $\mu = 2.0$ (see Fig.7), while $\mu = 2.0$ corresponds to a torus in the uncontrolled system.

Choosing $k = 0.091$, $\mu = 1.895$, in close vicinity to $\mu_{00} = 1.9$, we obtain a torus as predicted (see Fig.8). Here we note that for all the simulations of tori the initial conditions are $x_{10} = 0.1$, $x_{20} = 0.1$, $x_{30} = 0.1$ and the integral step is 0.05 in the Runge–Kutta Method.

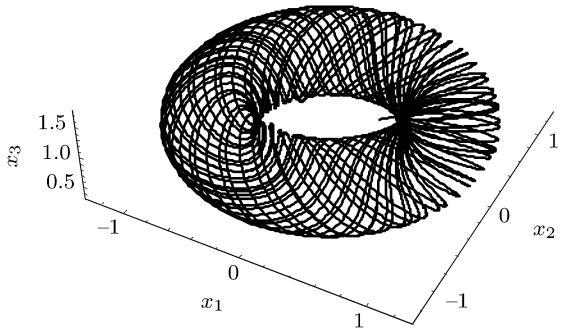


Fig.6. Tori of the controlled system (12) with $a = 3$, $b = 0.25$, $c = 0.2$ and $k = -0.074$, $\mu = 2.093$.

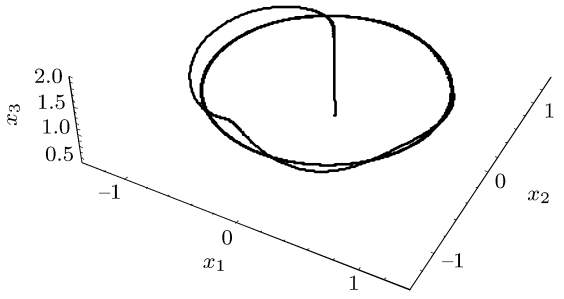


Fig.7. Limit cycle of the controlled Langford system (12) with $a = 3$, $b = 0.25$, $c = 0.2$ and $k = -0.074$, $\mu = 2.0$.

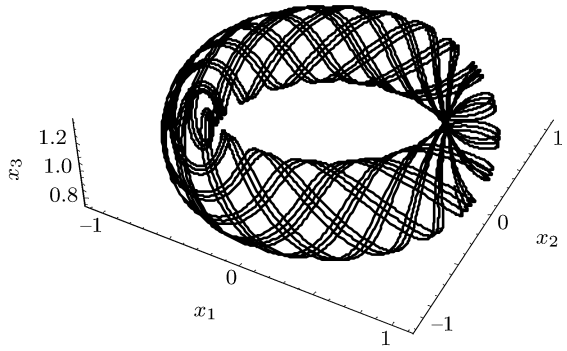


Fig.8. Tori of the controlled system (12) with $a = 3$, $b = 0.25$, $c = 0.2$ and $k = 0.091$, $\mu = 1.895$.

5. Conclusion

Bifurcation characteristics of the Langford system in a general form are systematically analysed and a nonlinear feedback controller is achieved to modify (delay or advance) its secondary Hopf bifurcation without changing the first Hopf bifurcation point. Analytical relationship between the bifurcation parameter and the control gain is explicitly obtained without any approximations by applying a polar coordinate transformation. Bifurcation diagrams are drawn showing the results of control for the secondary Hopf bifurcation and the sequences of bifurcations route to chaos. In the end quasi-periodic tori are numerically simulated to validate the analytic predictions.

References

[1] Iooss G 1975 *Arch. Rat. Mech. and Anal.* **58** 34
[2] Abed E H, Wang H O and Chen R C 1992 *Proc. IEEE Conf. Decis. Contr.* Tucson Artrona pp2119
[3] Langford W F 1979 *J. Appl. Math.* **37** 22
[4] Wen G L and Xu D L 2004 *Phys. Lett.* A **321** 24
[5] Wen G L and Wang Q G 2007 *Chaos, Solitons and Fractals* **34** 405
[6] Nikolov S and Petrov V 2004 *Int. J. Bifurcation and Chaos* **14** 293
[7] Chen G R, Moiola J L and Wang H O 2000 *Int. J. Bifurcation and Chaos* **10** 511
[8] Xiao H and Tang J S 2007 *Acta Phys. Sin.* **56** 101 (in Chinese)
[9] Tang J S, Fu W B and Li K A 2002 *Chin. Phys.* **11** 1004
[10] Rafilov M and Balthazar J M 2004 *Phys. Lett.* A **333** 241
[11] Li G H 2005 *Chin. Phys.* **14** 472
[12] Hopf E 1948 *Comm. Pure. Appl. Math.* **1** 303
[13] Hassard B, Kazarinoff N and Wan Y 1981 *Theory and Applications of Hopf Bifurcation* (London: Cambridge University Press)
[14] Nikolov S and Bozhkov B 2004 *Chaos, Solitons and Fractals* **21** 803
[15] Liu S H J and Tang J S 2007 *Acta Phys. Sin.* **56** 3145 (in Chinese)